



HAL
open science

Safety and Accuracy of Endovascular Aneurysm Repair Without Pre-operative and Intra-operative Contrast Agent

Adrien Kaladji, Aurélien Dumenil, Guillaume Mahé, Miguel Castro, Alain Cardon, Antoine Lucas, Pascal Haignon

► **To cite this version:**

Adrien Kaladji, Aurélien Dumenil, Guillaume Mahé, Miguel Castro, Alain Cardon, et al.. Safety and Accuracy of Endovascular Aneurysm Repair Without Pre-operative and Intra-operative Contrast Agent. *European Journal of Vascular and Endovascular Surgery Extra*, 2015, 49 (3), pp.255-261. 10.1016/j.ejvs.2014.12.003 . inserm-01108741

HAL Id: inserm-01108741

<https://inserm.hal.science/inserm-01108741>

Submitted on 23 Jan 2015

HAL is a multi-disciplinary open access archive for the deposit and dissemination of scientific research documents, whether they are published or not. The documents may come from teaching and research institutions in France or abroad, or from public or private research centers.

L'archive ouverte pluridisciplinaire **HAL**, est destinée au dépôt et à la diffusion de documents scientifiques de niveau recherche, publiés ou non, émanant des établissements d'enseignement et de recherche français ou étrangers, des laboratoires publics ou privés.

Safety and accuracy of endovascular aneurysm repair without preoperative and intraoperative contrast agent

Adrien Kaladji^{1,2,3}, Aurélien Dumenil^{2,3}, Guillaume Mahé^{3,4,5}, Miguel Castro^{2,3}, Alain Cardon¹, Antoine Lucas^{1,2,3} and Pascal Haigron^{2,3}

1. CHU Rennes, Centre of cardiothoracic and vascular surgery, F-35033 Rennes, France
2. INSERM, U1099, F-35000 Rennes, France
3. University Rennes 1, Signal and Image Processing Laboratory (LTSI), F-35000 Rennes, France
4. CHU Rennes, Imagerie coeur-vaisseaux, F-35033 Rennes, France
5. INSERM CIC-P 0203 Clinical investigation Centre Rennes, France

Corresponding author:

Adrien Kaladji, Centre of cardiothoracic and vascular surgery, University hospital of Rennes, F-35033 Rennes, France

Email: kaladrien@hotmail.fr

MANUSCRIPT

Introduction

Patients with renal impairment are problematic for endovascular therapists. Although frank renal failure is rare, it is common for progressive renal dysfunction to appear following endovascular aortic aneurysm repair(1) (EVAR). Patients undergoing EVAR are likely to have a pre-existing renal impairment, associated with their cardiovascular risk factors. Patients with severe renal failure or end-stage kidney failure are particularly exposed, following EVAR, to the short and medium-term risk of dialysis. Among the factors responsible for such complications, contrast-induced nephropathy(2, 3) (CIN) can be partly responsible for a deterioration in kidney function. CIN is defined as an increase in serum creatinine levels by ≥ 0.5 mg/dL, or $\geq 25\%$, with respect to the baseline value, within 72 hours following a contrast radiography using an iodinated contrast medium(4). CIN is more frequent in arterial procedures(5) and occurs in 2% to 25% of cases, following coronary procedures(6-8). One of the risk factors of CIN is pre-existing renal impairment. Permanent, severe renal failure requiring dialysis could occur in up to 10% of patients who have received a coronary angiography(9). Although the incidence of CIN in EVAR could be similar, this has not been accurately evaluated. Several techniques have been described, allowing the incidence of CIN to be reduced. One of these involves minimizing the volume of contrast medium, since the occurrence of CIN is dose-dependent. Current guidelines in cardiology(5) state that: “the volume of contrast media should be the minimum necessary to obtain adequate radiographs”. Fusion imaging is an emerging technique, facilitating navigation and visualization during EVAR. While fusion is associated with a significant reduction in the volume of injected contrast agent(10), this technique still requires the intraoperative injection of a minimal volume and, in particular, a pre-operative computerized tomography angiography (CTA). In the present paper, we describe a new image processing technique

allowing the preoperative CT-scan to be artificially enhanced. The resulting image can be used for the fusion imaging guidance of EVAR procedures, without the need for pre- and intraoperative contrast media. We report on the short-term results achieved with patients with severe chronic kidney disease (CKD).

Methods

The study protocol was approved by our institutional review board. Patient informed consent was obtained for being registered anonymously in our database. From October 2013 to February 2014, every patient requiring aortic aneurysm repair and presenting with an end-stage kidney failure (estimated glomerular filtration rate (eGFR) <15 ml/min/m²) or a severe renal failure (eGFR between 15 and 30 ml/min/m²) underwent pre-operative non-enhanced CT-scan and duplex scan imaging.

Pre-operative image analysis

The non-enhanced CT-scans were analysed with a dedicated 3D workstation (EndoSize(11), ThereNva). Centrelines were manually extracted by selecting points at the centre of the vessels (aorta, common iliac and renal arteries) using axial, coronal and sagittal views. A plane orthogonal to the centrelines was then created in order to measure their diameters. Five key points (P2 to P6) were positioned, allowing length measurements to be made and suitable endografts to be selected (Fig. 1).

A combination of several different image-processing functions allowed the pre-operative CT-scans to be virtually enhanced, using in-house software developed by the Signal and Image Processing Laboratory. Firstly, a set of contours was extracted by manually adjusting a B-spline curve (4 points) to the vessel lumen, in each of the cross-section planes (EndoSize). Using this technique, the contours extracted corresponded to the most external layer of the aorta (adventice). Secondly, from these curves, additional B-spline curves were created in the

longitudinal direction in order to build a “skeleton” of the vascular structure. The geometry of the vascular wall was then reconstructed by interconnecting the curves with a surface interpolation tool (Fig. 2) (Ansys DesignModeler). Finally, a binary volume with the same properties as the patient's CT-scan (dimensions, spacing...) was generated by rasterizing the mesh representing the vascular structure. The original patient CT-scan was then modified to enhance the contrast between the vascular structure and the surrounding tissues, by artificially increasing the value of the vascular structure voxels to 500 Hounsfield Units (HU) (Fig. 3). This method enhanced every voxels within the contours initially extracted and could not separate thrombus and vessel lumen. Vessel centreline (aorta, iliac and renal arteries) and key point representations were then added to the patient CT-scan, using the same method. A 3 mm diameter cylindrical mesh was used for the centrelines, and a larger diameter (5 mm) spherical mesh was used for the key points. These additional features were included in the CT-scan, through the use of density values lying outside the range of those corresponding to human tissues (> 3000 HU).

Intraoperative imaging

The surgical procedures were performed in the TheraImage Plateform Angiosuite at the Rennes University Hospital, France. The virtually enhanced pre-operative CT-scan was then imported into the Syngo software (Siemens Healthcare, Forchheim, Germany). In order to construct the fusion image, this software was used to match the pre-operative CT-scan with an intraoperative Cone Beam CT, recorded with a 270° c-arm rotation (Artis Zeego; Siemens Healthcare). The methodology used to construct this type of fusion image has been fully described in previous papers(12, 13), and was also applied in the present study. This process allowed the virtually enhanced 3D vascular volume, including the centrelines and key points, represented by different colours (Fig. 4), to be projected onto the 2D live fluoroscopic image. The alignment of this projection was checked at the beginning of the procedure, by

catheterizing the lowest renal artery with a 0.014 inch guidewire, which was later retrieved. For the thoracic case, the left subclavian artery was catheterized with the same method. Following completion of the procedure, the patency of the aortic collaterals, the effective exclusion of the aneurysm, and the absence of any endoleak, were verified by an experienced radiologist using a duplex scan. For the thoracic case, a cardiologist came at the end of the procedure to perform a transesophageal duplex ultrasound.

Post-operative imaging

A second duplex scan and a non-enhanced CT scan were performed before discharge, and again one month later (duplex scan only). For the thoracic case, a second transesophageal duplex was performed before discharge but not at one month (only CT scan). To assess the accuracy of the stent-graft deployment, specific distances were measured, identifying the proximal and distal landing zones on the pre- and post-operative scans. In the case of abdominal aneurysms, the distance (L1 pre) between the lowest renal artery and the planned landing zone (key point P2) was measured, in addition to the distance (L2 pre) between the origin of the internal iliac artery and the planned distal landing zone (key points P5 and P6). In the case of thoracic aneurysm, these distances were measured between the subclavian artery and the proximal landing zone, and between the coeliac trunk and the distal landing zone. On the post-operative CT scan, the same measurements were performed: the distance (L1 post) between the top of the endograft (identified by gold markers) and the planned proximal landing zone (pre-operative key point P2); and the distance (L2 post) between the planned distal landing zone (key points P5 and P6) and the end of the endograft, were measured.

The differences between “L1 pre” and “L1 post”, and between “L2pre” and “L2 post”, were therefore considered to be the errors in stent-graft placement at the proximal and distal landing zones, respectively.

Statistical analysis

The data are presented as mean standard deviations for the quantitative variables, unless otherwise noted. The non-parametric Wilcoxon signed rank test was used to compare the variations in serum creatinine and eGFR levels.

Results

Six patients (one woman and five men, mean age 77.1 years) were treated for endovascular aneurysm repair (5 abdominal aneurysms and 1 descending thoracic aneurysm). The patients' demographic characteristics and pre-operative anatomic measurements are provided in Table 1. The mean preoperative serum creatinine level (Scr) and eGFR was 295 $\mu\text{mol/l}$ and 19.6 ml/min/1.73 m^2 respectively.

The procedures were performed under general anaesthesia. The percutaneous approach was used in all cases. Two Endurant, 2 Cook LP, and 1 Gore Excluder C3 stent-grafts were used. The technical success rate of these interventions was 100%. No contrast medium was used during any of the procedures. The mean fluoroscopic time was 21.1 min, and the mean radiation dose area was 8.1 mGy.m^2 . No intraoperative endoleak was observed on the post-operative duplex scan nor on those performed before discharge. The patient with a thoracic aneurysm was treated with a Valient Captivia delivery system, deployed below the subclavian artery and 45 mm above the celiac trunk. No endoleak was observed on transesophageal duplex.

The post-operative follow-up was free of complications in all cases. The mean length of hospital stay was 5.2 days. The variations in eGFR and serum creatinine levels are provided in Table 2. No significant variation in Scr/eGFR was observed at 3 days (mean Scr/eGFR=280/20.5), at 1 week (mean Scr/eGFR=301/19.2) and at 1 month (mean Scr/eGFR =322/18.7). One patient required definitive dialysis at 35 days follow-up, in the context of a

coronary endovascular revascularization for an acute coronary syndrome. One type 2 endoleak was noted on the patient's duplex scan at 1 month follow-up. The mean stent-graft placement errors at the proximal and distal landing zones were 1.33 mm and 6.5 mm, respectively. The details of the various reference distances measured in each patient are presented in Table 3.

Discussion

CIN is not as infrequent as commonly believed. In addition to acute kidney failure, patients developing CIN are also more exposed to adverse long-term events (14). It is thus indispensable that new techniques be developed, in an effort to reduce the use of contrast media during endovascular procedures. Canyigit et al.(15) have described the catheterization of the lowest renal artery during EVAR, with a mean contrast volume of 47 ml. This technique is simple, but still requires the use of a contrast medium. Alternatives to iodinated contrast agents, such as carbon dioxide (CO₂), have been proposed. As a consequence of respiratory elimination, CO₂ has no side effect on renal function, and the safety of its use in EVAR has been reported in several studies(16-18). Although no deterioration in renal function was reported in these studies, some of the data is contradictory. Whereas Chao et al.(16). reported longer fluoroscopy and operating room times, and increased radiation exposure, Criado et al.(17) observed the opposite effect. Recently, a prospective study(18) was conducted to assess the use of CO₂ for the detection of endoleaks in EVAR. In this study, the iodinated contrast agent appears to lead to better results than CO₂. Moreover, the widespread utilization of CO₂ is limited by the difficulties associated with its use: a dedicated injector is required, and most practitioners are unfamiliar with the administration protocol. Finally, the use of CO₂ leads to a risk of ischemia, resulting from the presence of undissolved gas in the bloodstream(19).

Fusion imaging is an emergent technology, which has been introduced into vascular surgery, and is practiced in hybrid rooms. This application can be used in computed-assisted surgery(20), thereby providing valuable information at the appropriate moment, contributing to decision making, and enhancing the security of endovascular procedures. Two studies(10, 21) have revealed a significant reduction in the use of contrast media during complex endovascular aneurysm repair, and Kobeiter et al.(22) have reported the first zero contrast agent endovascular aneurysm repair to be achieved with fusion imaging. Concerning X-ray exposure, some of the results are contradictory(21, 23), thus calling for confirmation of these preliminary outcomes. McNally et al(24) recently reported a significant decrease of all intraoperative data during fenestrated procedure: X-ray exposure, procedure time and contrast usage. From our own experience (>100 EVAR carried out in a hybrid room), X-ray exposure in the hybrid room is greater than in a standard operating room, but also depends on the use of c-arm equipment.

The use of fusion imaging with a non-enhanced pre-operative CT has not been previously described. The advantage of our process is that it leads to an overlay of not only the 3D aortic volume, but also the sizing information. In the first case treated by our team, since the neck diameter was irregular it was decided to deploy the endograft 11 mm below the lowest renal artery. By overlaying key sizing points (P2), it was thus possible to respect the planning. Although the pre-operative image processing required the participation of a team experienced in the use of this technology, it is now possible to apply this software process to any non-enhanced CT-scan. The implementation of this software clearly has no side effects, and specific skills are no longer required during the procedure. Fusion with pre-operative magnetic resonance angiography (MRA) has also been reported, for the treatment of an internal iliac aneurysm(25). The sizing procedure for EVAR with MRA imagery is more complex. However, the pre-operative fusion of an MRA image and a non-enhanced CT-scan

(then used for intraoperative fusion) could be an advantageous solution for patients with CKD.

Our protocol has some limitations. The process requires manual contouring of the aorta on the non-injected scan. This step is assisted by the software, but nevertheless takes approximately 30 minutes. The whole process is therefore difficult to use in emergency situations. This technology is not currently available elsewhere than in our centre. The long-term outcome of procedures using this technology remains to be determined. As mentioned in the description of the technique, the artificial enhancement cannot assess the location of the thrombus. But we usually size EVAR adventice to adventice, so thrombus is therefore no important. Even though there was thrombus at the proximal neck, these patients would underwent EVAR because they were deemed unfit for open repair. The detection of any endoleak after completion of the procedure could be underestimated, because the ultrasound techniques dedicated to vascular procedures could be less sensitive than those used during follow-up examinations. Nevertheless, radiologists have confirmed that a significant endoleak can be realistically detected, even with the ultrasound devices commonly employed in vascular procedures. The positional errors in stent-graft placement reported in our study are reasonable. Even when procedures are carried out with a contrast agent, this parameter is rarely measured. The distal landing zone errors are greater than the proximal landing zone errors, which can be explained by the deformation of iliac arteries resulting from the use of stiff guidewires. There are differences in the iliac artery lengths, between those measured on the pre-operative CT-scan and those measured during procedures. This discrepancy can lead to accidental hypogastric coverage, and we are currently evaluating the use of numerical simulations to anticipate such deformations(26).

Conclusion

In the present study, we describe the first known implementation of an EVAR procedure

without the use of any pre- or intraoperative contrast agents. This was achieved through the use of specific software applied to fusion imaging. The artificial enhancement of CT-scans is a new process, among various alternatives to the use of iodinated contrast agents, and is intended for the case of patients with severe CKD. Long-term results with a larger cohort are needed, before the accuracy of this technology can be confirmed.

Acknowledgments

The authors are indebted to the Centre of Clinical Investigation and Technological Innovation 804 for its support in the processing of the imaging data.

This study was carried out at the experimental TherA-Image platform (Rennes, France), and was supported by Europe FEDER.

References

1. Walsh SR, Tang TY, Boyle JR. Renal consequences of endovascular abdominal aortic aneurysm repair. *J Endovasc Ther.* 2008;15(1):73-82.
2. Rundback JH, Nahl D, Yoo V. Contrast-induced nephropathy. *J Vasc Surg.* 2011;54(2):575-9.
3. Solomon R. Contrast media nephropathy--how to diagnose and how to prevent? *Nephrol Dial Transplant.* 2007;22(7):1812-5.
4. Solomon R, Dauerman HL. Contrast-induced acute kidney injury. *Circulation.* 2010;122(23):2451-5.
5. Ohno I, Hayashi H, Aonuma K, Horio M, Kashihara N, Okada H, et al. Guidelines on the use of iodinated contrast media in patients with kidney disease 2012: digest version : JSN, JRS, and JCS Joint Working Group. *Clin Exp Nephrol.* 2013;17(4):441-79.
6. Ahuja TS, Niaz N, Agraharkar M. Contrast-induced nephrotoxicity in renal allograft recipients. *Clin Nephrol.* 2000;54(1):11-4.
7. Chou SH, Wang ZJ, Kuo J, Cabarrus M, Fu Y, Aslam R, et al. Persistent renal enhancement after intra-arterial versus intravenous iodixanol administration. *Eur J Radiol.* 2011;80(2):378-86.
8. Lufft V, Hoogestraat-Lufft L, Fels LM, Egbeyong-Baiyee D, Tusch G, Galanski M, et al. Contrast media nephropathy: intravenous CT angiography versus intraarterial digital subtraction angiography in renal artery stenosis: a prospective randomized trial. *Am J Kidney Dis.* 2002;40(2):236-42.
9. Scanlon PJ, Faxon DP, Audet AM, Carabello B, Dehmer GJ, Eagle KA, et al. ACC/AHA guidelines for coronary angiography. A report of the American College of Cardiology/American Heart Association Task Force on practice guidelines (Committee on

- Coronary Angiography). Developed in collaboration with the Society for Cardiac Angiography and Interventions. *J Am Coll Cardiol*. 1999;33(6):1756-824.
10. Tacher V, Lin M, Desgranges P, Deux JF, Grunhagen T, Becquemin JP, et al. Comparison of Two-dimensional (2D) Angiography, Three-dimensional Rotational Angiography, and Preprocedural CT Image Fusion with 2D Fluoroscopy for Endovascular Repair of Thoracoabdominal Aortic Aneurysm. *J Vasc Interv Radiol*. 2013.
 11. Kaladji A, Lucas A, Kervio G, Haigron P, Cardon A. Sizing for endovascular aneurysm repair: clinical evaluation of a new automated three-dimensional software. *Ann Vasc Surg*. 2010;24(7):912-20.
 12. Dijkstra ML, Eagleton MJ, Greenberg RK, Mastracci T, Hernandez A. Intraoperative C-arm cone-beam computed tomography in fenestrated/branched aortic endografting. *J Vasc Surg*. 2011;53(3):583-90.
 13. Kaladji A, Dumenil A, Castro M, Haigron P, Heautot JF, Haulon S. Endovascular aortic repair of a postdissecting thoracoabdominal aneurysm using intraoperative fusion imaging. *J Vasc Surg*. 2013;57(4):1109-12.
 14. Solomon RJ, Mehran R, Natarajan MK, Doucet S, Katholi RE, Staniloae CS, et al. Contrast-induced nephropathy and long-term adverse events: cause and effect? *Clin J Am Soc Nephrol*. 2009;4(7):1162-9.
 15. Canyigit M, Cetin L, Uguz E, Algin O, Kucuker A, Arslan H, et al. Reduction of iodinated contrast load with the renal artery catheterization technique during endovascular aortic repair. *Diagn Interv Radiol*. 2013;19(3):244-50.
 16. Chao A, Major K, Kumar SR, Patel K, Trujillo I, Hood DB, et al. Carbon dioxide digital subtraction angiography-assisted endovascular aortic aneurysm repair in the azotemic patient. *J Vasc Surg*. 2007;45(3):451-8; discussion 8-60.

17. Criado E, Upchurch GR, Jr., Young K, Rectenwald JE, Coleman DM, Eliason JL, et al. Endovascular aortic aneurysm repair with carbon dioxide-guided angiography in patients with renal insufficiency. *J Vasc Surg.* 2012;55(6):1570-5.
18. Huang SG, Woo K, Moos JM, Han S, Lew WK, Chao A, et al. A prospective study of carbon dioxide digital subtraction versus standard contrast arteriography in the detection of endoleaks in endovascular abdominal aortic aneurysm repairs. *Ann Vasc Surg.* 2013;27(1):38-44.
19. Nadolski GJ, Stavropoulos SW. Contrast alternatives for iodinated contrast allergy and renal dysfunction: options and limitations. *J Vasc Surg.* 2013;57(2):593-8.
20. Kaladji A, Lucas A, Cardon A, Haigron P. Computer-aided surgery: concepts and applications in vascular surgery. *Perspect Vasc Surg Endovasc Ther.* 2012;24(1):23-7.
21. Sailer AM, de Haan MW, Peppelenbosch AG, Jacobs MJ, Wildberger JE, Schurink GW. CTA with fluoroscopy image fusion guidance in endovascular complex aortic aneurysm repair. *Eur J Vasc Endovasc Surg.* 2014;47(4):349-56.
22. Kobeiter H, Nahum J, Becquemin JP. Zero-contrast thoracic endovascular aortic repair using image fusion. *Circulation.* 2011;124(11):e280-2.
23. Hertault A, Maurel B, Sobocinski J, Martin Gonzalez T, Le Roux M, Azzaoui R, et al. Impact of Hybrid Rooms with Image Fusion on Radiation Exposure during Endovascular Aortic Repair. *Eur J Vasc Endovasc Surg.* 2014.
24. McNally MM, Scali ST, Feezor RJ, Neal D, Huber TS, Beck AW. Three-dimensional fusion computed tomography decreases radiation exposure, procedure time, and contrast use during fenestrated endovascular aortic repair. *J Vasc Surg.* 2014.
25. Sadek M, Berland TL, Maldonado TS, Rockman CB, Mussa FF, Adelman MA, et al. Use of preoperative magnetic resonance angiography and the Artis zeego fusion program to

minimize contrast during endovascular repair of an iliac artery aneurysm. *Ann Vasc Surg.* 2014;28(1):261 e1-5.

26. Kaladji A, Dumenil A, Castro M, Cardon A, Becquemin JP, Bou-Said B, et al. Prediction of deformations during endovascular aortic aneurysm repair using finite element simulation. *Comput Med Imaging Graph.* 2013;37(2):142-9.

Fig. 1 Non injected 3D aortic volume. For sizing and planning 5 keys points are placed: proximal landing zone (P2) ; end of proximal neck (P3) ; aortic bifurcation (P4), right and left distal landing zone (P5, P6)

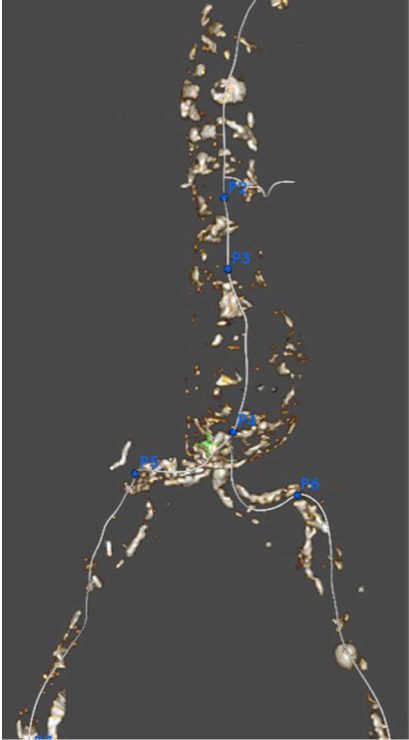


Fig. 2 From the CT-scan, contours of the aorta are exported in a software (Ansys DesignModeler) allowing a connection between them with a surface interpolation tool.

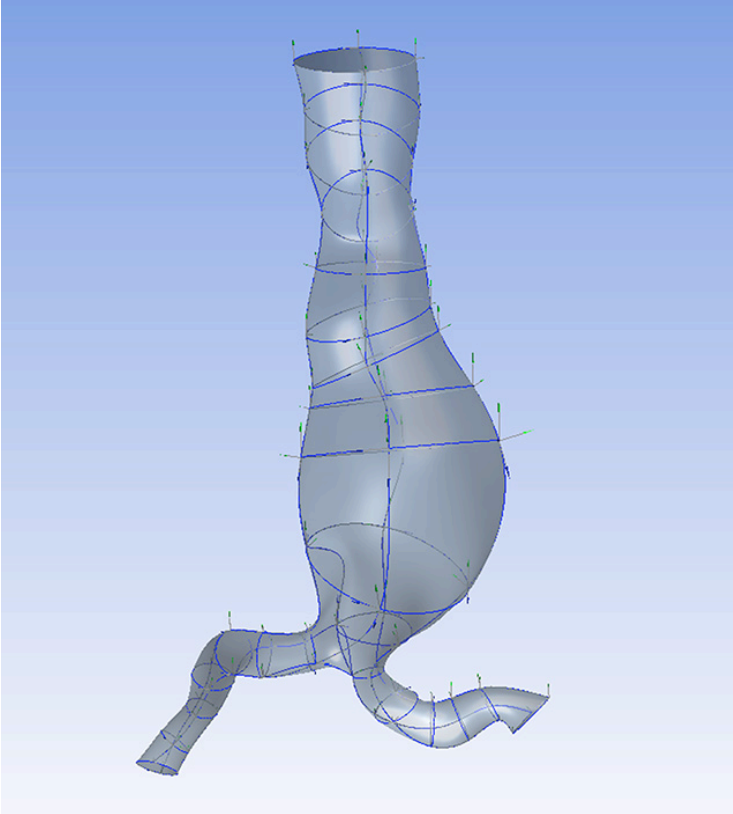


Fig. 3 Preoperative CT-scan before (A,C) and after (B,D) artificial enhancement on axial view (A, B) and on 3D view (C,D). Centerlines are added to the 3D view (D) and external iliac arteries not represented.

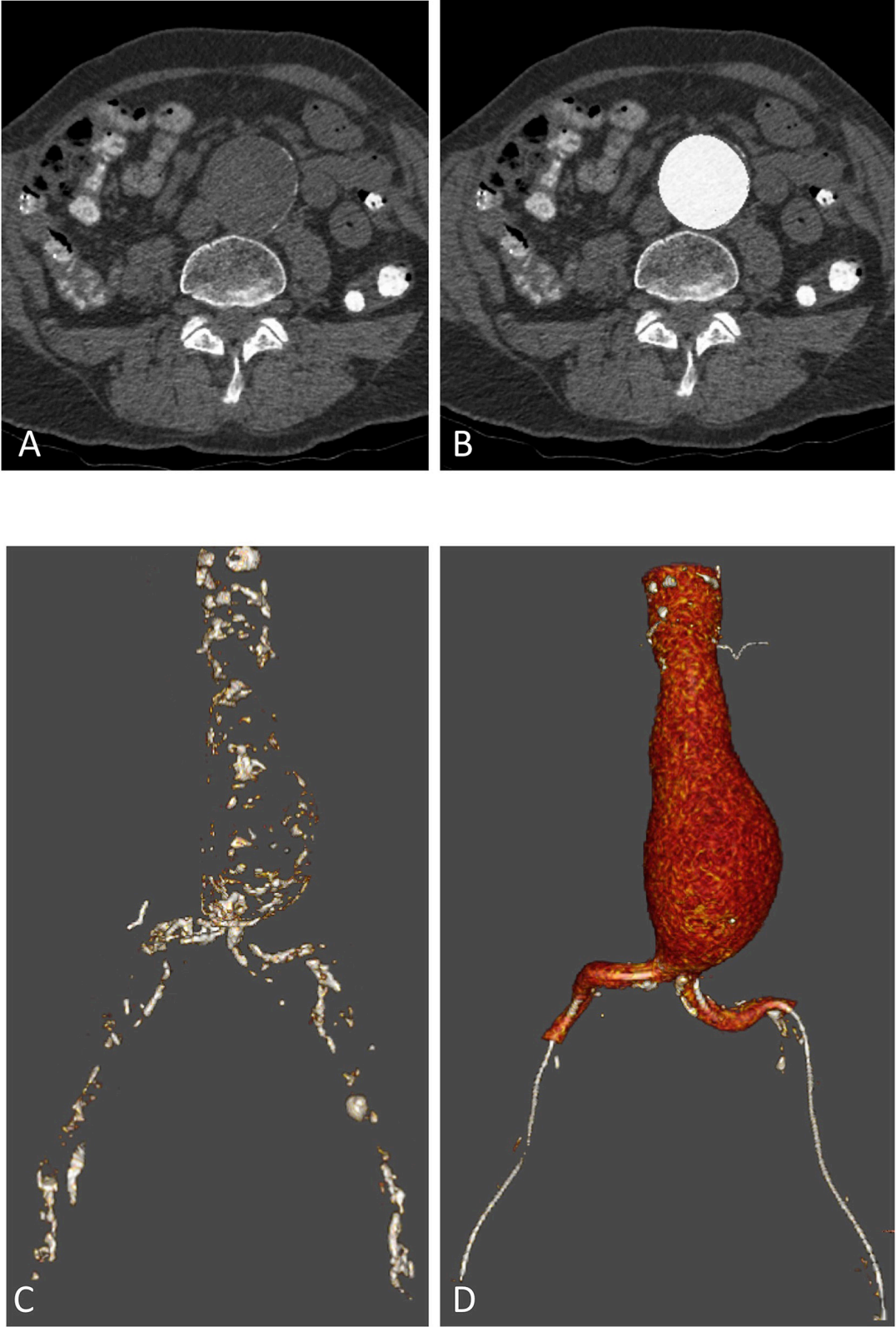


Fig.4: During the procedure, different information can be overlaid onto the native 2D fluoroscopic image (A). Centerlines and keys points can be projected (B), as the artificially enhanced aortic volume.

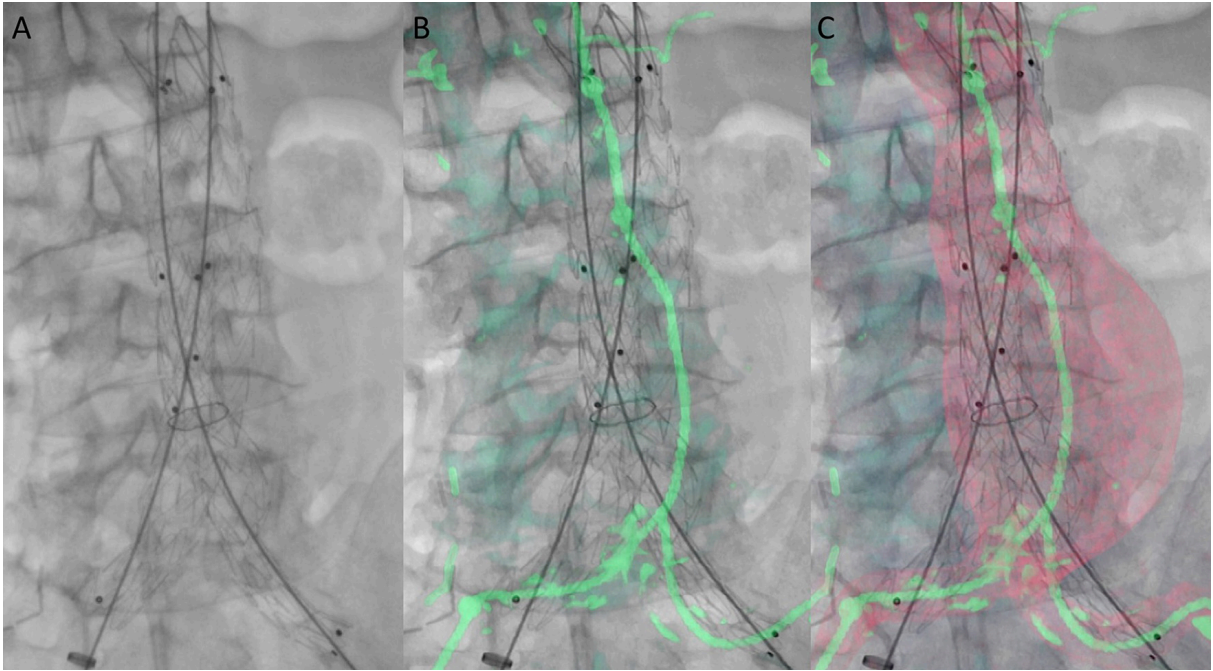


Table 1 Patients' characteristics and intraoperative data.

	Patient 1	Patient 2	Patient 3	Patient 4	Patient 5 (t)*	Patient 6
Age (years)	80	74	79	87	84	62
Aneurysm diameter (mm)	54	52	43**	55	65	51
Neck length (mm)	35	15	34	38	35	17
Fluoroscopic time (min)	24.2	20.8	24.3	9.1	15.1	33
Dose area product (mGy/m ²)	13.8	10.5	5	6.2	5.7	7.1

* patient with a descending thoracic aneurysm

**patient with a false aneurysm

Table 2. eGFR at baseline, 3 days after the procedure, and at 1 month follow-up.

	Patient 1	Patient 2	Patient 3	Patient 4	Patient 5	Patient 6	P value**
Pre-operative Scr/eGFR	355/15	291/19	347/12	190/30	375/14	210/28	
3 days post-operative Scr/eGFR	313/18	260/22	356/11	202/28	332/16	214/28	0.4/0.34
1 week post-operative Scr/eGFR	425/12	277/20	304/14	192/29	389/13	220/27	0.75/0.59
1 month post-operative Scr/eGFR	553/10*	277/20	307/14	190/29	376/14	230/25	0.79/0.5

Scr Serum creatinine level (μmol/l), eGFR estimated glomerular filtration rate (ml/min/1.73m²)

*Patient requiring definitive dialysis in the context of endovascular coronary revascularization

** p value from the Wilcoxon signed rank test comparing preoperative Scr/eGFR with the 3 days, 1 week and 1 month data

Table 3. Distances used for the assessment of stent-graft placement accuracy.

	Patient 1	Patient 2	Patient 3	Patient 4	Patient 5 (t)*	Patient 6
L1 pre (mm)	11	0	12	0	0	0
L1 post (mm)	11	1	14	3	2	0
Stent-graft placement error at proximal landing zone (mm)	0	1	2	3	2	0
L2 pre (mm) (r/l) **	5/16	0/0	19/22	8/6	56	4/10
L2 post (mm) (r/l)**	26/15	12/11	24/17	6/6	45	5/18
Stent-graft placement error at distal landing zone (mm)	21/1	12/11	5/5	2/0	5	1/8

L1 pre: distance between the lowest renal artery and key point P2

L1 post: distance between the lowest renal artery and the proximal extremity of the endograft

L2 pre: distance between the origin of the internal iliac artery and the key points P5 (right) or P6 (left)

L2 post: distance between the origin of the internal iliac artery and the extremity of the limb endograft

* patient with a descending thoracic aneurysm, distances were measured between the subclavian artery and the proximal landing zone (L1 pre and post), and between the coeliac trunk and the distal landing zone (L2 pre and post)

** right distal landing zone/left distal landing zone